A robust field-based method to screen heat tolerance in wheat

Najeeb Ullah[1], Jack Christopher[1], Troy Frederiks[2], Shangyu Ma[1,3], Daniel KY Tan[4], Karine Chenu[1,*]

[1] The University of Queensland, Queensland Alliance for Agriculture and Food Innovation (QAAFI), Leslie Research Facility, 13 Holberton street, Toowoomba, QLD 4350, Australia

[2] Department of Agriculture and Fisheries, 203 Tor street, Toowoomba, QLD 4350, Australia

[3] School of Agronomy, Anhui Agricultural University, Hefei, Anhui, China

[4] The University of Sydney, Plant Breeding Institute, Sydney Institute of Agriculture, School of Life and Environmental Sciences, Faculty of Science, Sydney, NSW 2006, Australia

[*] Corresponding author: karine.chenu@uq.edu.au

Abstract

Wheat crops are highly sensitive to elevated temperatures, particularly during pollen meiosis and early grain filling. As the impact of heat stress greatly depends on the developmental stage of a crop, wheat germplasm ranking for heat tolerance in field experiments may be confounded by variation in developmental phase between genotypes at the time of heat events. Deploying an artificial-photoperiod-extension method (PEM) has allowed screening of diverse genotypes at matched developnemtal phases during natural heat events despite phenological varations. Irrigated experiments with 32 wheat genotypes were conducted in south-east Queensand, Australia with either (i) the PEM or (ii) conventional field plots. The paired PEM and conventional field plot trials were sown at different?? with serial sowing dates from June to September. In the PEM, plants were sown in single rows or in small plots and artificial supplemental lighting was installed at one end of each row/plot, extending day length to 20 h close to the lights. The intensity of supplementary lighting diminished as the distance from the lights increased, and induced a gradient of flowering times along each row/plot. Spikes of each genotype were tagged when they flowered. Late-sown crops received more heat shocks during early and/or mid-grain filling than earlier sowings, and suffered significant yield losses. Significant genotypic differences in heat tolerance ranking were observed between PEM versus conventional plot screening. Individual grain weight of the tested wheat genotypes was strongly correlated in the PEM plots experiencing a similar degree of heat, but the correlation was either poor or negative in conventional plot trials. With PEM, we successfully quantified the impact post-flowering heat on individual grain weight of wheat genotypes with the heat events occurring precisely at a specific developmental stage. The PEM results produced robust field based rankings of genotypes for heat tolerance within trials experiencing similar heat events. This

method promises to improve the efficiency of heat tolerance field screening, particularly when comparing genotypes of different maturity types.

Keyword: Phenotyping, heat stress, genotype x environment interaction, crop improvement, photoperiod extension.

Introduction

Climate variability is among the major determinants of global crop yields, including wheat (Najeeb et al., 2019; Ray et al., 2015) and strongly impedes plant breeding (Chapman et al., 2012). A significant increase in the frequency of extreme temperatures, particularly during grain filling has been recorded in the major wheat production regions such as Australia during the past 30 years (Ababaei and Chenu, 2020). These extreme heat events have substantially affected the growth, development and ultimately, yield of wheat crops (e.g. Collins et al., 2021; Collins and Chenu, 2021; Zheng et al., 2016). With the recent rate of climate change, a further increase in the frequency of these heat events is projected in the near future both in Australia (Ababaei and Chenu, 2020) and globally (Field et al., 2012). Thus, developing wheat genotypes with superior heat tolerance during grain filling is critical for sustaining wheat grain yields and maintaining food security in future hot climates.

Wheat crops are highly sensitive to elevated temperatures with the impact of heat stress is highly dependent on the crop developmental stage (e.g. Chenu and Oudin, 2019; Farooq et al., 2011; Prasad and Djanaguiraman, 2014). Reproductive and grain filling phases of wheat crops are extremely sensitive to heat and even a mild increase in the atmospheric temperature during these stages can significantly reduce grain yield. For example, high temperature during double-ridge stage significantly damages spikelet primordia development reducing the potential grain number (Slafer and Rawson, 1994). Similarly a single hot day (>30◦C) during early reproductive stage during the onset of meiosis in pollen or micro / megaspore development, can completely sterilise the developing wheat pollen (Saini and Aspinall, 1982). The effect of high temperature on pollen typically translates into a poor grain set and grain yield loss (Guo et al., 2016). Each degree increase (from 15–22°C) in mean temperature during pollen developmental can reduce grain number per unit area by 4%, while 10°C increase in maximum temperature at mid anthesis can result in a 40% reduction in grain number in wheat spikes (Wheeler et al., 1996).

Post-anthesis heat reduces grain yield primarily by limiting assimilate synthesis, translocation, and starch deposition to developing grains (Sofield et al., 1977). Grain weight

is most sensitive to heat during early grain filling and becomes progressively less sensitive as grain filling proceeds (Stone and Nicolas, 1998). A single hot day (maximum day temperature 40°C) occurring 10–13 days after anthesis can reduce individual grain weight (IGW) by 14% (Stone and Nicolas, 1998). With each day delay in exposure to heat stress during this period (15-35 days after anthesis), 0.5% reduction in individual grain weight of wheat has been recorded (Stone and Nicolas, 1998). Reduction in individual grain weight of heat stressed plants is strongly linked with a shortened grain filling duration ((Girousse et al. 2021; Stone and Nicolas, 1998); Girousse et al., 2021) and for each °C rise in temperature above optimum (15–20°C), a two to eight day reduction in grain filling duration has been reported in wheat crop (reviewed by Streck, 2005). In the Australian wheatbelt, a steady increase in the frequency of hot days (T_{max} > 26°C) during the grain filling period of wheat crops has been recorded over the past 30 years (Ababaei and Chenu, 2020). With grain yield losses largely the results of reduced grain weight (18.1%) rather than reduced grain number (3.6%). This highlights the importance of developing wheat germplasm more tolerant to heat post-flowering.

Conventionally, wheat genotypes are screened for heat tolerance by serial sowing, using heat chambers in the field, or in controlled environments (Thistlethwaite et al., 2020). Ranking for heat tolerance is typically based on physiological or morphological traits associated with plant function and performance (Bennett et al., 2012). However, changes in these traits are strongly influenced by the environment and the methodology used (Limpens et al., 2012; Poorter et al., 2016). Field-based screening methods are generally considered more representative of the plant response to natural environments (Passioura, 2006). However, screening of wheat genotypes with varying maturity types may be further complicated by the unpredictability of heat events under field conditions. Given that the impact of heat events is highly dependent on the developmental phase specific in wheat test line (e.g. Chenu and Oudin, 2019; Djanaguiraman et al., 2014; Tashiro and Wardlaw, 1990), ranking of wheat genotypes for heat tolerance may be confounded by variation in developmental stage during a natural heat event. An improved technique to screen for high temperature stress at matched developmental stages of wheat genotypes in the field could accelerate the selection of heat tolerant genotypes.

Here, we developed and tested an artificial-photoperiod-extension method (PEM) that allows comparison of the performance of wheat genotypes with varying maturity types at a common

100 developmental stage during natural heat events. The method was tested across three different
101 locations over three consecutive years. Rankings of wheat genotypes with varying maturity
102 type and heat tolerance were compared using PEM and conventional plots.

103 **Materials and Methods**

104 *Growth conditions and experimental design*

105 Field experiments were conducted over three consecutive years (2018 to 2020) at three
106 locations across southern Queensland, Australia. Conventional serial sowing field plots were
107 estabilished adjacent trials using a newly developed photoperiod extension method (PEM).
108 Randomised block design experiments with two times of sowing blocks and four replicates
109 were established each year. To maximise the likelihood of heat during grain filling, the
110 experiments were planted later in the cropping season than industry practice (Table 1). The
111 first sowings (s1) were established between late May or early July and the second sowings
112 (s2) between late August or early September at The University of Queensland Research
113 Farm, Gatton (27°34′50″S, 152°19′28″E). At the Hermitage Research Station, Warwick
114 (28°12'40"S, 152°06'06"E), experiments were sown early June or mid-July (s1) or mid-
115 August and mid-September (s2). At the Tosari Crop Research Centre, Tummaville
116 (27°49'09.1"S 151°26'14.9"E), the crops were sown mid-July (s1) and early September (s2).
117 All experiments were fully irrigated at sowing (except at Tosari) and cultivated under non-
118 limiting fertiliser conditions (Table 1). A boom irrigator (centre pivot sprinkler) was used for
119 irrigating plot trials at Gatton and Tosari, while wobbler sprinklers were set up for irrigating
120 PEM trials at Gatton and Hermitage (in 2018). In 2020, both PEM and plots trials at the
121 Hermitage were irrigated using a drip irrigation system. At Tosari, the crops were irrigated at
122 sowing and pre-flowering, but no post flowering irrigation was applied. Standard crop
123 management practices including weed, disease and pest control were adopted during the
124 season.

125 With the PEM method, wheat genotypes were either hand sown in a 5 m single row in 2018
126 and 2019 or machine planted in a four row plot (1×5 m, 2020).

127 Conventional field plots were planted at the same time and with similar management to the
128 PEM trials. In 2018 and 2020, the conventional yield (2×6 m) plots were set up in Gatton and
129 Hermitage, while in 2019 genotypes were tested in smaller plots (1×6 m) at Tosari and
130 Gatton. All conventional plots were planted at a 25 cm row spacing with a population density
131 of 130 plants m^{-2} and in four independent replications.

132 *Genotypes*

133 Thirty-five wheat (*Triticum aestivum* L.) genotypes with contrasting phenology and
134 adaptation (Table S1, supplementary) were used in the study. These included three high-
135 performing spring cultivars Suntop, Mace and Scout widely cultivated in the northern,
136 western, and southern regions of Australia, respectively. A set of eight CIMMYT genotypes
137 described as heat tolerant under Australian environments was obtained from the University of
138 Sydney (Thistlethwaite et al., 2020). Other genotypes used in these experiments included
139 donors of a multi-reference parent nested association mapping (NAM) population developed
140 for screening for drought tolerant wheat (Christopher et al., 2015, 2021; Richard, 2017). In
141 total, 35 wheat genotypes were tested under PEM and plot experiments, with 32 genotypes
142 each year and site, except PEM plots in 2020 when only 20 selected genotypes were used
143 (Table S1, Supplementary). In conventional plot experiments, 32 genotypes were used each
144 year.

145 *The photoperiod extension method*

146 The novel photoperiod extension method (PEM), was based on a method described by
147 Frederiks et al. (2012) to test for frost damage and was adapted to for screening wheat
148 genotypes for heat tolerance under field conditions. At one end of each row or plot, LED
149 lamps (CLA LT401, 9W T40 LED LAMP, 3000K 760LM) with a lumen efficiency ≥ 80,
150 were set up approximately 1 m above the ground level and at spacing of 0.8 m. These lamps
151 supplement light as the sunset by extending the day length to 20 h (Fig. 1). The intensity of
152 light diminishes with the square of the distance from the lights along test row, with maximum
153 effect closest to the lights and minimum or no impact at the other end of the row. This
154 variation in light intensity across the rows induced a gradient of flowering times within each
155 row with the plants closest to the light developing more rapidly.

156 *Plant measurements*

157 For each PEM trial and sowing date in 2018 and 2019, approximately 20 stems of the each
158 genotypes were tagged at flowering (Zadoks decimal growth stage 65; Zadoks et al., 1974).
159 The induced gradient in phenology along the rows allowed tagging of genotypes multiple
160 times for plants in rows or plots from each sowing time. One-to-three cohorts of stems at
161 precisely matched for developmental stage at flowering (Zadoks decimal growth stage 65
162 were tagged in rows or plots from each sowing time and location. These sequentially tagged
163 coherts were termed as tagging 1, tagging 2 and tagging 3. The tagged spikes were manually

harvested at maturity and processed for grain yield components. In addition, in each test row, a 0.5 m section of row that originally contained the heads from first tagging was manully harvested for harvest index and crop yield estimation. In 2020, ~ 0.5 m section of each plot was tagged at flowering (Zadoks 65), and two centr0al rows (0.5 m each) within the tagged region were manually harvested at crop maturity.

All yield plots from the conventional method were harvested using a small plot amchine harvester at maturity when grain moisture was approximately 11%. Grain samples were maunally counted to calculate individual grain weight (IGW).

Environment variables

Local weather stations (Campbell Scientific) were set up at each site to record weather data. Light sensors (Apogee SP-110 pyranometers, and Apogee SQ-110 for radiation and PAR measurements, respectively) were installed at 1.5 m height, collecting light interception data for each 10 min. period. Average daily intercepted radiations (mean daily radiations (MJ m^{-2}) are presented (Table 1). HMP60 (Vaisala INTERCAP®) probes were used for air temperature (Tair) and relative humidty (RH) measurements installed 1.5 high.

Thermal time was calculated in degree days using the following equation:

$$Degree\ days = -0.0032 * Tair^3 + 0.1369 * Tair^2 + 0.3968 * Tair + 0.993 \quad \text{(Eq 1)}$$

Where Tair is the hourly air temperature data

Day-time vapour pressure deficit (VPD) was calculated as in (Alduchov and Eskridge, 1996), by the following equation

$$VPD = 0.61094\left(\frac{1-RH}{100}\right)^{17.625*\mathrm{Tair}/(\mathrm{Tair}+243.04)} \quad \text{(Eq 2)}$$

Where Tair and RH are the hourly air temperature and hourly relative humidity, respectively, during the daytime.

Statistical analysis

Data were analysed using R (Team, 2018). Individual and interaction effects of genotype and environments (sowing, location and tagging), were determined by analysis of variance (ANOVA). Statistical differences were tested with student's t-tests at a 5% level (Condon et al., 2004). Principal component analysis was computed to rank genotypes in different environments.

Results

Wheat crops experienced a wide range of heat events across locations and sowing times

Wheat genotypes at each location, season, sowing and tagging experienced varying air temperatures and VPD (vapour pressure deficit) in the pre- and post-flowering periods (Table 1, Fig. 2 & Table S2 supplementary data). In all trials, the plants from sowing 2 experienced significantly higher temperatures and VPD than crops from the first sowing. For example, post-flowering mean air temperature was 20% higher for s2 than s1 crops across the trials (Table 1). Similar differences in post-flowering maximum air temperature of s1 and s2 crops were also observed, with the exception of in the 2020 Warwick trial (WAR20), where the difference between the maximum temperature during s1 and s2 was only 10%. The number of hot days (with max temperature >30°C) across these experiments also varied greatly, with second sowing (s2) in 2019 receiving the maximum number (22) of post flowering hot days. Higher temperature during s2 shortened the duration of both pre- and post-flowering periods, although the reduction in time to flowering was relatively greater than the reduction in post-flowering duration across all the tested locations (Table 1).

At TOS19, crops received pre-flowering supplementary irrigation, but water was unavailable for post-flowering irrigation. Thus, these crops experienced a degree of post-flowering drought. With optimal pre flowering temperature (Table S2, supplementary data), s1 plant at TOS19 produced potential number of grains (spike^{-1}) but significant reduction in grain size was confounded by post-flowering heat and drought.

Table 1. Field experiment environmental characteristics and management including the trial identifier (Trial), site, irrigation treatment and sowing date. Also presented are the mean of pre- and post-flowering periods, as well as post-flowering temperature, day-time vapour pressure deficit (VPD) and radiation for experiments with photoperiod extension method (PEM). Days to flowering and grain filling duration were calculated from sowing to flowering and flowering to maturity, respectively, for the 1st tagging 1 (T1) at each location and sowing time.

Trial *	Site	Irrigation	Sowing date	Mean temp. (°C)	Mean daily max temp. (°C)	Mean VPD (kPa)	Mean daily radiation (MJ m^{-2})	Days to flowering (days)	Post-flowering duration (days)	Days with post-flowering max temp. >30°C
GAT18s1	Gatton	Full**	03/07/2018	19.3	26.3	0.74	23.8	73	42	1
GAT18s2	Gatton	Full	31/08/2018	23.1	31.4	1.38	23.2	53	39	11
WAR18s1	Warwick	Full	16/07/2018	18.6	25.6	0.84	17.7	73	39	2
WAR18s2	Warwick	Full	12/09/2018	22.0	30.3	1.52	21.2	52	37	9
GAT19s1	Gatton	Full	09/07/2019	19.5	28.7	1.40	16.8	71	39	5
GAT19s2	Gatton	Full	03/09/2019	23.7	33.8	2.23	20.8	59	35	20
TOS19s1	Tummaville	Supplementary	16/07/2019	21.1	30.2	1.26	17.7	79	35	12
TOS19s2	Tummaville	Supplementary	06/09/2019	26.5	36.7	2.27	16.2	62	35	22
GAT20s1	Gatton	Full	26/05/2020	17.9	26.8	1.08	17.3	79	49	0
GAT20s2	Gatton	Full	04/08/ 2020	22.2	31.2	1.35	19.7	65	37	14
WAR20s1	Warwick	Full	08/06/ 2020	19.3	26.3	0.74	13.6	73	42	1
WAR20s2	Warwick	Full	12/08/2020	23.1	31.4	1.38	11.6	53	39	4

GAT18s1 and GAT18s2, sowing 1 and sowing 2 at Gatton in 2018, respectively; GAT19s1 and GAT19s2, sowing 1 and sowing 2 at Gatton in 2019, respectively; GAT20s1 and GAT20s2, sowing 1 and sowing 2 at Gatton in 2020, respectively; WAR18s1 and WAR18s2, sowing 1 and sowing 2 at Warwick in 2018, respectively; WAR20s1 and WAR20s2, sowing 1 and sowing 2 at Warwick in 2019, respectively; TOS19s1 and TOS19s2, sowing 1 and sowing 2 at Tummaville in 2018, respectively.

TOS19 crops had supplementary pre-flowering irrigation and had experienced a mild post-flowering water stress.

Late-sown crops had lower individual grain weight and grain yield

Individual grain weight and grain yield significantly varied across experiments but generally s2 crops produced significantly smaller grains and lower grain yield compared with s1 crops (Fig. 3). No significant variation in grain number (spike^{-1}) of the tested wheat genotypes were observed in this study, except s2 trials of TOS19 and GAT19 (Table S8, Supplementary data), where significant pre-flowering heat events (Fig. 2) impacted the grain set.

The wheat genotypes (averaged across all tested genotypes) produced maximum IGW (44.7 mg grain^{-1}) and grain yield (516 g m^{-2}) under PEM-GAT18s1. Across the plots, genotypes produced maximum IGW (37.7 mg grain^{-1}) and grain yield of (478 g m^{-2}) under WAR20s1. Trial-mean reduction in IGW between s2 and s1 crops were maximum at GAT19 for PEM (71%) and conventional plot trials (32%) (Fig 3a & c). In contrast, grain yield reduction varied across PEM and conventional plots i.e. grain yield loss in s2 compared with s1 was maximum at GAT18 and TOS19 for PEM and conventional plots, respectively (Fig 3b & d).

Extending the photoperiod with lights increased opportunities to tagged plants from contrasting genotypes at matched development stage, especially in earlier sown crops

Phenology data were collected from plants 0.5 m from each end and of each experimental row or plot in the PEM, from next to the supplemented light or at the far end away from the supplemental lights (Fig. 4-5). The phenology of the different genotypes significantly varied both under natural and supplemented light. The supplemented light accelerated flowering by 8.5 days (164 growing degree days) and 5.6 days (120 growing degree days) on average in s1 and s2 crops, respectively. This gap between flowering times of plants under natural and supplemented light allowed multiple tagging of the genotypes at matched developmental phases (Zadok 65 in this study) within rows or plots from single time of sowing.

Supplemented light had a weaker effect in late sowings when the natural photoperiod was already longer (Fig. 5). Under the shortest studied photoperiods (~10.5 h at sowing), plants closer to the light source flowered approximately 8 days earlier than the plants away from light source (averaged across genotypes and sites). The phenology effect of supplemented light nearly halved when crops were planted under longer photoperiod (11.5 h or more at sowing).

A reduction in individual grain weight by 1.5 mg for every post-flowering heat day

A strong correlation (r^2 = 0.903) between the number of post-flowering hot days (days with maximum temperature >30°C) and individual grain weight was observed across PEM plots (Fig. 6a). This suggested that number of post-flowering hot days is a critical determinant of the final grain weight of wheat crops.

Plots receiving 0-4 post flowering hot days, produced largest grains (40-45 g grain^{-1}). Given that heat event (if any) during these plots were very brief (~30 min, Fig. 2), IGW produced during this period was categorised as potential grain weight. In contrast, GAT19s2 and TOS19s2 experienced significant pre- and post- flowering heat (i.e. more than 20 post flowering hot days) and suffered maximum reduction in grain size. On average, plants under these extremely hot plots produced 2.7 times smaller grains than the potential IGW (Fig. 6a).

Plots with intermediate/a moderate numbers of heat events i.e. 5 - 13 post flowering hot days and showed significant variations in mean grain weights and grain yield. On average, IGW of the tested wheat genotypes in HET2 trials was reduced by 2.1 mg for every post-flowering heat day. Similarly, significant variations in mean grain weights were observed among different tagging within a single sowing time, particularly when plants experienced varying number of hot days. For instance, m2 plants of GAT19s1 produced 14% smaller grains compared with m1 plants.

The photoperiod-extension method provided a stable genotype ranking within heat environment type

Genotypic rankings with the PEM were consistent between environments experiencing similar heat stress (Fig. 7). Trials were divided in three heat environment types (HET; Fig. 6): HET1 corresponded to environments with no or only late grain-filling heat stress (i.e. less of 4 cumulated hours of temperature >30°C between 0 and 500°Cd after flowering), HET2 included all environments with moderate heat stress during grain fill (5 to 13 days with a maximum temperature >30°C in our set of trials), and HET3 corresponded to environments severely stressed during grain fill (20 to 22 days with a maximum temperature >30°C in our set of trials). In addition to post flowering heat, HET3 trials experienced high pre flowering temperatures (Table S2) along with multiple hot days around stem elongation and meiosis (Fig. 2). These pre flowering heat shocks significantly reduced the grain set (Fig S1, supplementary data).

For single spike harvests with the PEM, correlations for the plants experiencing mild or no heat stress during grain-filling (maximum temperature >30°C between 0 and 500°Cd after flowering), i.e. HET1, ranged from 0.64 to 0.89 (Figure 2 & 7a). A range of positive correlations (excluding TOS19 which experienced a degree of post flowering drought) were observed for the moderately-stressed environments within HET2. These correlations were stronger (r^2 = 0.57-0.9) among the irrigated trials with a similar number of hot days (i.e. 9-13) and became more variable with the trial with five hot days only (i.e. r^2=0.2-0.57). A wide range of positive correlations was also observed among HET1 and HET2 trials, the strength of these correlations varied with the number of hot days observed in trials. IGW of the two severely-stressed trials (HET3) was strongly correlated (r^2 = 0.46) but correlations between HET3 and HET1 or HET2 trials varied (Fig 7a).

IGW data collected from a PEM row meter was also positively correlated between different trials, and these correlations were particularly strong among the trials experiencing a similar number of hot days, Fig. 7b. For example, in HET1 these correlations were moderate to strong (r^2=0.24-0.88) mainly because of a weaker correlation between GAT20s1 and WAR20s1 (r^2 = 0.24). Similarly, all HET2 trials were positively correlated except drought-stressed trial (i.e. TOS19s1).

In the conventional method, based on comparison from plots sown at different sowing dates, genotype ranking for IGW varied widely across the environments, both between sowings and sites (Fig. 7c). Correlations were positive mainly under optimum environments, i.e. 0-4 hot days, but they were poor and sometimes negative across other environments. A maximum correlation of 0.78 was found between GAT20s1 and WAR20s1, with 0-2 hot days during grain filling. HET2 trials were either poorly or even negatively correlated i.e. GAT19s1 has a strong correlation (r^2 = 0.48) only with TOS19s. Similarly, HET3 trials GAT19s2 and TOS19s2 had a correlation of 0.1.

Irrigated trials were also positively correlated for grain yield (g m^{-2}) data collected from row harvest in PEM trials. The correlations ranged (r^2 = 0.2-0.72) and (r^2 = 0.33-0.63) under HET1 and HET2, respectively (Fig. S2, supplementary data). Under conventional plots, correlations for grain yield were either poor or negative for most of these trials.

IGW grain weight data collected from the two trial methods were also compared. A strong positive correlation (r^2=0.94) was observed between the IGW data collected under PEM trials by collecting single spike or by row meter harvest (Fig. 8a). In contrast, when IGW data of row meter harvest and plot trials are plotted, this correlation was poor (r^2=0.147) and non-significant, except between GAT18s2 trials (Fig. 8b & Fig. S4, supplementary data).

The photoperiod extension method allows a distinct clustering of wheat genotypes across the tested environments

Performance of wheat genotypes in terms of IGW and grain yield (grain weight g spike^{-1} for spike harvest data) for the studied environments were explored using principle component analysis (PCA) biplots. The first two principle components (PC) explained maximum variance (~ 60% for IGW and grain yield across different trial types), thus the data from PC1 and PC2 are presented here (Fig. 9).

Under PEM, a strong positive correlation was observed between HET1 (GAT18s1 and WAR18s1) and HET2 (GAT18s2 and WARs2) trials, except TOS19s1 (Fig. 9 a & d). This correlation was stronger within HETs (site, sowing and tagging). In contrast, a wider angle between HET3 (GAT19s2 and TOS19s2) and HET1/HET2 for IGW and HET1 for grain weight loadings suggested a weaker correlation between these trials (Fig. 9 a & d).

The projection of a genotype onto an environmental axis reflects the performance of that genotype in that environment. Based on their performance in different environments, the tested genotypes were grouped together. Biplot separated the tested genotypes into three distinct groups for IGW and grain weight (spike^{-1}) under different environments (Fig. 9 a & d). For instance, the top performing genotypes such as ZWB10-37 project axis above the origin in HET1 and HET2 and show a positive interaction with these environments (green ellipse, Figure 9). In contrast, poorly performing genotypes such as Yitpi and EGA Wylie project below the origin on the same axis (red ellipse, Figure 9).

For the row meter harvest of the PEM, PC loadings of HET1 and HET2 were also positively correlated particularly for IGW (Fig. 9 b & e). Clustering of genotypes based on their performance in the different environments was distinct both for IGW and grain yield (Figure 9).

Under conventional plots, environment types (HET), particularly for grain yield were more widely separated, indicating a weaker or even negative correlation among them (Fig. 9c & f). Compared with PEMs, genotype ranking was also greatly changed in the conventional plots. For instance, genotypes such as RIL114, EGA Gregory and Suntop_1 were ranked among the top performing genotypes for IGW under some of HET1 and HET2 (Fig. 9c). This ranking under the plot trials was further complicated when the tested genotypic performance was compared for grain yield under plot trials (Fig. 9f).

Discussion

A new method to screen for heat tolerance at matched development stages

The reproductive developmental stages of wheat are highly susceptible to elevated temperatures, with heat events heat events can significantly impair grain set and final grain size. During the grain filling phase, sensitivity of developing grains to heat events can change over a period a short as a few days (Stone and Nicolas, 1995). Since field-based techniques for screening heat tolerant germplasm generally rely serial sowing, it is hard to optimise sowing time for given the unpredictable timing of heat events. Field-based screening for heat tolerance using this conventional method is further complicated when genotypes with varying maturity types are tested together. These genotypes are likely to receive heat events across different developmental stages with heat escape confounding true heat tolerance. Thus, for yield assessments, the development of plots needed to be synchronised and timed to occurrence during heat events, which is hard to achieve in practice (Single, 1991).

We developed a new method, which allows screening of wheat genotypes at matched developmental phases with greater flexibility in the timing of natural heat events. As quality and quantity (photon flux density) of intercepted light determine phenological development in wheat (Fischer and Stockman, 1980), we manipulated wheat phenology by altering the intensity of intercepted light. This was achieved using supplemental lights, which extended photoperiod at one end of the test rows to 20 h. The light intensity diminishes with the square of distance (Niinemets and Keenan, 2012), generating a series of flowering times along the length of the test rows (Fig. 1). The range of flowering times within a single row of individual genotype, allowed tagging and comparison of the performance of genotypes with varying maturity types at precisely matched developmental stages (flowering). The impact of supplemented light for phenology manipulation was complemented by using a wide range of sowing dates from late May to mid-September. Our study showed that the impact of extended photoperiod is strongly (r^2=0.54) associated with the natural photoperiod during vegetative crop growth. For instance, a wide gap in flowering across the test rows, of up to 10 days when averaged across all tested genotypes, was recorded in the crops planted during longer (photoperiod ≥11.50 h) and this gap narrowed by 3.5 days with each increasing hour in photoperiod at sowing (cite data figures and tables). In our PEM plots, a wider flowering time gradient allows multiple tagging within a single time of sowing improving the efficiency to trials. Thus, if resources are limited a single sowing at, or a bit later than the first sowing times used in this study may be sufficient for reliable screening of a range of spring habit test

wheat lines. Arguably, s2 was planted too late in the season and receive too many heat events to be representative i.e. HET3 in our experiments, it may be hard to accurately rank genotypes using PEM.

Our study demonstrated that heat intensity during the grain filling period of irrigated wheat are the major determinant final grain size and grain yield. A threshold maximum daily temperature of 30°C was critical during grain filling phase of wheat crops (Porter and Gawith, 1999). In this study, tested wheat genotypes did not experience any significant IGW or grain yield loss in response to 0-4 hot days (max daily temperature >30°C) during grain filling (HET1, Fig. 6). This could be because most of these heat events were either very brief (1-2 h only, Fig. 1) or the heat event occurred late in development when grain-filling was already well advanced (Fig. 2).

Significant variation in the timing and intensity of natural heat events across sowing times and locations were recorded and consequently the effect on grain yield was highly variable in the conventional system (Fig. 2 & 3). Our data showed that reduction in IGW was highly influenced by the intense and number of heat shocks during early to mid-grain filling (HET2). A significant and strong effect of the timing of heat has also been recorded on grain weight of wheat during this sensitive period under controlled environmental conditions (Stone and Nicolas 1996)**.**

In this study, each additional hot day during grain filling (HET2) reduced IGW of tested wheat genotypes was by 1.57 mg (Fig. 6a). Interestingly, this significant (p<0.001) reduction in IGW was also recorded with plants exposed to varying heat in a single sowing. For example, in the Gatton 2019 first sowing (GAT19 s1) plants tagged one week later (tagging 2) experienced four additional days of post flowering heat and consequently produced 14% smaller grains than tagging 1 (Fig. 6). Developmental phase-specific effects of heat shocks (particularly in HET2) on grain yield of wheat genotypes were observed in this study (Fig. 6) highlighting the importance of screening wheat germplasm at matched developmental phases.

The PEM method allows reliable ranking of wheat genotypes under varying environments

Strong correlations among different trials for IGW and grain yield with PEM (Fig. 7 a & c, S1, supplementary data) indicated a stable ranking of tested genotypes particularly within the environments receiving a similar degree of heat (Tables S3,S4 & S6 Supplementary data). For instance, the mean correlations for IGW of wheat genotypes across irrigated HET1, HET2 and HET3 trials were 0.81, 0.59 and 0.57, respectively, under PEM. In contrast, these

correlations were strong for HET1 (r^2=0.57) but poor for HET2 (r^2=0.11) and HET3 (r^2=0.1) using conventional yield plots (Table S5 & S7 Supplementary data). This indicate that in conventional plots, ranking wheat genotypes was changed depending on the number of hot days, particularly during early grain filling (i.e. HET2). High heat sensitivity during this developmental phase has also been reported by Talukder et al. (2013), who observed a single hot day (maximum temperature > 35°C) during this period can significantly reduce grain weight of wheat crops.

The stable genotype ranking within similar environments is also evident from the proximity of principal component (PC) loading in PEM trials (Figure 9). Despite variable correlations among various HET trials, PEM allowed the tested genotypes to be clustered into distinct groups based on their performance in these environments (Fig. 9a & d). In contrast, this clustering was inconsistent with that found in conventional plots. The clustering in the conventional plots was also much less powerful at separating groups of genotypes as seen by the greater overlap of genotypes within each group (Figure 9e). This indicates that the PEM reliably ranked wheat genotype across a wide range of hot environments compared to the conventional plots. Given that the magnitude, timing and duration of heat strongly influences final grain weight in wheat (Stone and Nicolas, 1996; Tewolde et al., 2006), genotypes of contrasting maturity could experience varying intensity of post flowering when tested together in the conventional method. For instance, wheat genotypes tested in one of our trials GAT18s2, flowered at from 53 to 64 days after sowing (Fig. 4). In this trial, genotypes tagged at matched developmental stage in tagging 1 and 2 received a significant heat spike (maximum temperature >35°C) at 8 and 15 days after flowering, respectively (Fig. 2) and thus experienced different degree of damage. However, late flowering genotypes of GAT18s2 which were not flowering and so not tagged genotypes in the conventional plot trial could experience heat events significantly later (up to 11 days) than the quick flowering genotypes and consequently avoided heat stress. This indicates that genotype ranking for heat tolerance in conventional plots is prone to be more unreliable under HET2, where heat events occurred more frequently during early to mid-grain filling (Fig. 2) as well as in the projected future environment across Australia (Ababaei and Chenu, 2020).

Implications for breeding

A high throughput and accurate method for screening heat tolerance is necessary for sustaining food security under changing environments, particularly for the projected hot and dry environments. In our PEM experiments, we tested the performance of wheat genotypes

using single row and small plots. The plants were tagged either as individual spikes or as row segments (50 cm) of the plot at a matched developmental stage. Our data suggest that the most reliable genotype ranking can be achieved by tagging and harvesting individual spikes at matched developmental stage (Fig. 7 and 9). The PEM method described could be suited for fine tuning the ranking of subset of selected genotypes in the field, as the data from field grown plants are often more reliable than conventional controlled environment studies. Our study suggests that tagging part of a row or plot at a matched developmental phase give highly robust data. This could potentially be used for large number of genotypes in the breeding programs with further adaptation of the method. Strong positive correlations between IGW (r^2=0.94) and grain weight (r^2=0.51) of spike and row meter harvest as observed in this study (Fig. 6, Fig. S1 and S2 Supplementary data) suggested that wheat genotypes can be reliably screened with plot sowing with quadrat (~50 cm) harvest.

In our PEM trials, number of post-flowering hot days were strongly correlated (r^2 = 0.90) with and grain weight per spike (Fig. 6 a & b) but not with the grain number per spike (r^2 = 0.01). This strongly suggests that grain yield reductions in these irrigated trials, particularly in HET1 and HET2 were mainly the consequence of grain weight loss due to post-flowering heat stress rather than changes in grain number. With the projected increase in frequency and intensity of post flowering heat across the Australian wheatbelt (Ababaei and Chenu, 2020), the PEM described here offers an opportunity to select for heat tolerant wheat genotypes more reliably than can be done conventionally.

Conclusions

We developed and tested a new field-based method for screening wheat genotypes for heat tolerance under natural heat events. In this method, we used supplemental light to manipulate crop phenology in a way that genotypes with varying phenology could be tested at closely matched developmental stages when a heat event occurred. Significantly, strong correlation with the number (r^2=0.84) and timing (r^2=0.89) of post flowering hot days were observed in the PEM trials emphasised the importance of screening wheat genotypes at a matched developmental stage. With this method, we successfully quantified genotype × environment response for the heat events occurring precisely at a specific developmental stage. This method also allowed the comparison of genotype performance at multiple developmental stages within a single sowing time or location. The method provided robust heat tolerance ranks for the genotypes tested in similar heat-stress environments. This method promises to

improve the efficiency of heat tolerance field screening, particularly when comparing genotypes of different maturity types.

Acknowledgments

The research was made possible thanks to the support of The University of Queensland and the Queensland Government, Department of Agriculture and Fisheries. Najeeb Ullah was supported by a Queensland Government, Advance Queensland Fellowship. We acknowledge and thank Ian Broad (Department of Agriculture and Fisheries Queensland) for assistance operating weather stations across the studied sites and Thaís Helena Godoy Sanches for sample processing and data collection.

References

Ababaei, B., Chenu, K., 2020. Heat shocks increasingly impede grain filling but have little effect on grain setting across the Australian wheatbelt. Agric. For. Meteorol. 284, 107889. https://doi.org/10.1016/j.agrformet.2019.107889

Alduchov, O.A., Eskridge, R.E., 1996. Improved Magnus form approximation of saturation vapor pressure. J. Appl. Meteorol. https://doi.org/10.1175/1520-0450(1996)035<0601:IMFAOS>2.0.CO;2

Bennett, D., Reynolds, M., Mullan, D., Izanloo, A., Kuchel, H., Langridge, P., Schnurbusch, T., 2012. Detection of two major grain yield QTL in bread wheat (Triticum aestivum L.) under heat, drought and high yield potential environments. Theor. Appl. Genet. https://doi.org/10.1007/s00122-012-1927-2

Chapman, S.C., Chakraborty, S., Dreccer, M.F., Howden, S.M., 2012. Plant adaptation to climate changeopportunities and priorities in breeding, in: Crop and Pasture Science. https://doi.org/10.1071/CP11303

Chenu, K., Oudin, F., 2019. Heat impact on yield components of fertile primary tillers in wheat can inform crop modelling for future climates 23–26.

Christopher, J., Richard, C., Chenu, K., Christopher, M., Borrell, A., Hickey, L., 2015. Integrating Rapid Phenotyping and Speed Breeding to Improve Stay-Green and Root Adaptation of Wheat in Changing, Water-Limited, Australian Environments. Procedia Environ. Sci. https://doi.org/10.1016/j.proenv.2015.07.246

Christopher, M., Paccapelo, V., Kelly, A., Macdonald, B., Hickey, L., Richard, C., Verbyla, A., Chenu, K., Borrell, A., Amin, A., Christopher, J., 2021. QTL identified for stay-green in a multi-reference nested association mapping population of wheat exhibit context dependent expression and parent-specific alleles. F. Crop. Res. 270, 108181. https://doi.org/10.1016/j.fcr.2021.108181

Collins, B., Chapman, S., Hammer, G., Chenu, K., 2021. Limiting transpiration rate in high evaporative demand conditions to improve Australian wheat productivity. in silico Plants. https://doi.org/10.1093/insilicoplants/diab006

Collins, B., Chenu, K., 2021. Improving productivity of Australian wheat by adapting sowing date and genotype phenology to future climate. Clim. Risk Manag. https://doi.org/10.1016/j.crm.2021.100300

Condon, A.G., Richards, R.A., Rebetzke, G.J., Farquhar, G.D., 2004. Breeding for high water-use efficiency, in: Journal of Experimental Botany. https://doi.org/10.1093/jxb/erh277

Djanaguiraman, M., Vara Prasad, P. V., Murugan, M., Perumal, R., Reddy, U.K., 2014. Physiological differences among sorghum (Sorghum bicolor L. Moench) genotypes under high temperature stress. Environ. Exp. Bot. https://doi.org/10.1016/j.envexpbot.2013.11.013

Farooq, M., Bramley, H., Palta, J.A., Siddique, K.H.M., 2011. Heat stress in wheat during reproductive and grain-filling phases. CRC. Crit. Rev. Plant Sci. 30, 491–507. https://doi.org/10.1080/07352689.2011.615687

Field, C.B., Barros, V., Stocker, T.F., Dahe, Q., Jon Dokken, D., Ebi, K.L., Mastrandrea, M.D., Mach, K.J., Plattner, G.K., Allen, S.K., Tignor, M., Midgley, P.M., 2012. Managing the risks of extreme events and disasters to advance climate change adaptation: Special report of the intergovernmental panel on climate change, Managing the Risks of Extreme Events and Disasters to Advance Climate Change Adaptation: Special Report of the Intergovernmental Panel on Climate Change. https://doi.org/10.1017/CBO9781139177245

Fischer, R., Stockman, Y., 1980. Kernel Number Per Spike in Wheat (Triticum aestivum L.): Responses to Preanthesis Shading. Funct. Plant Biol. https://doi.org/10.1071/pp9800169

Girousse, C., Inchboard, L., Deswarte, J., Chenu, K., 2021. How does post-flowering heat impact grain growth and its determining processes in wheat□? Environ Exp Bot

Guo, Z., Slafer, G.A., Schnurbusch, T., 2016. Genotypic variation in spike fertility traits and ovary size as determinants of floret and grain survival rate in wheat. J. Exp. Bot. 67, 4221–4230. https://doi.org/10.1093/jxb/erw200

Limpens, J., Granath, G., Aerts, R., Heijmans, M.M.P.D., Sheppard, L.J., Bragazza, L., Williams, B.L., Rydin, H., Bubier, J., Moore, T., Rochefort, L., Mitchell, E.A.D., Buttler, A., van den Berg, L.J.L., Gunnarsson, U., Francez, A.J., Gerdol, R., Thormann, M., Grosvernier, P., Wiedermann, M.M., Nilsson, M.B., Hoosbeek, M.R., Bayley, S., Nordbakken, J.F., Paulissen, M.P.C.P., Hotes, S., Breeuwer, A., Ilomets, M., Tomassen, H.B.M., Leith, I., Xu, B., 2012. Glasshouse vs field experiments: Do they yield ecologically similar results for assessing N

impacts on peat mosses? New Phytol. https://doi.org/10.1111/j.1469-8137.2012.04157.x

Najeeb, U., Tan, D.K.Y., Sarwar, M., Ali, S., 2019. Adaptation of crops to warmer climates: Morphological and physiological mechanisms, in: Sustainable Solutions for Food Security: Combating Climate Change by Adaptation. https://doi.org/10.1007/978-3-319-77878-5_2

Niinemets, Ü., Keenan, T.F., 2012. Measures of light in studies on light-driven plant plasticity in artificial environments. Front. Plant Sci. https://doi.org/10.3389/fpls.2012.00156

Passioura, J.B., 2006. The perils of pot experiments. Funct. Plant Biol.

Poorter, H., Fiorani, F., Pieruschka, R., Wojciechowski, T., van der Putten, W.H., Kleyer, M., Schurr, U., Postma, J., 2016. Pampered inside, pestered outside? Differences and similarities between plants growing in controlled conditions and in the field. New Phytol. https://doi.org/10.1111/nph.14243

Porter, J.R., Gawith, M., 1999. Temperatures and the growth and development of wheat: A review. Eur. J. Agron. https://doi.org/10.1016/S1161-0301(98)00047-1

Prasad, P.V.V., Djanaguiraman, M., 2014. Response of floret fertility and individual grain weight of wheat to high temperature stress: Sensitive stages and thresholds for temperature and duration. Funct. Plant Biol. https://doi.org/10.1071/FP14061

Ray, D.K., Gerber, J.S., Macdonald, G.K., West, P.C., 2015. Climate variation explains a third of global crop yield variability. Nat. Commun. https://doi.org/10.1038/ncomms6989

Richard, C., 2017. Breeding wheat for drought adaptation: Development of selection tools for root architectural traits. https://doi.org/10.14264/uql.2017.1055

Saini, H., Aspinall, D., 1982. Sterility in Wheat (Triticum aestivum L.) Induced by Water Deficit or High Temperature: Possible Mediation by Abscisic Acid. Funct. Plant Biol. https://doi.org/10.1071/pp9820529

Slafer, G.A., Rawson, H.M., 1994. Does temperature affect final numbers of primordia in wheat? F. Crop. Res. https://doi.org/10.1016/0378-4290(94)90013-2

Sofield, I., Evans, L., Cook, M., Wardlaw, I., 1977. Factors Influencing the Rate and Duration of Grain Filling in Wheat. Funct. Plant Biol. https://doi.org/10.1071/pp9770785

Stone, P.J., Nicolas, M.E., 1998. The effect of duration of heat stress during grain filling on two wheat varieties differing in heat tolerance: Grain growth and fractional protein accumulation. Aust. J. Plant Physiol. https://doi.org/10.1071/PP96114

Stone, P.J., Nicolas, M.E., 1996. Effect of timing of heat stress during grain filling on two wheat

varieties differing in heat tolerance. II. Fractional protein accumulation. Aust. J. Plant Physiol. https://doi.org/10.1071/PP9960739

Stone, P.J., Nicolas, M.E., 1995. Effect of timing of heat stress during grain filling on two wheat varieties differing in heat tolerance. I. Grain growth. Aust. J. Plant Physiol. https://doi.org/10.1071/PP9950927

Streck, N.A., 2005. Climate change and agroecosystems: the effect of elevated atmospheric CO2 and temperature on crop growth, development, and yield. Ciência Rural. https://doi.org/10.1590/s0103-84782005000300041

Talukder, A.S.M.H.M., McDonald, G.K., Gill, G.S., 2013. Effect of short-term heat stress prior to flowering and at early grain set on the utilization of water-soluble carbohydrate by wheat genotypes. F. Crop. Res. 147, 1–11. https://doi.org/10.1016/j.fcr.2013.03.013

Tashiro, T., Wardlaw, I., 1990. The Response to High Temperature Shock and Humidity Changes Prior to and During the Early Stages of Grain Development in Wheat. Funct. Plant Biol. https://doi.org/10.1071/pp9900551

Team, R.C., 2018. R Development Core Team. R: A language and environment for statistical computing. R Foundation for Statistical Computing, Vienna, Austria; 2014. Google Sch.

Tewolde, H., Fernandez, C.J., Erickson, C.A., 2006. Wheat cultivars adapted to post-heading high temperature stress. J. Agron. Crop Sci. https://doi.org/10.1111/j.1439-037X.2006.00189.x

Thistlethwaite, R.J., Tan, D.K.Y., Bokshi, A.I., Ullah, S., Trethowan, R.M., 2020. A phenotyping strategy for evaluating the high-temperature tolerance of wheat. F. Crop. Res. https://doi.org/10.1016/j.fcr.2020.107905

Wheeler, T.R., Batts, G.R., Ellis, R.H., Hadley, P., Morison, J.I.L., 1996. Growth and yield of winter wheat (Triticum aestivum) crops in response to CO2 and temperature. J. Agric. Sci. https://doi.org/10.1017/s0021859600077352

ZADOKS, J.C., CHANG, T.T., KONZAK, C.F., 1974. A decimal code for the growth stages of cereals. Weed Res. https://doi.org/10.1111/j.1365-3180.1974.tb01084.x

Zheng, B., Chenu, K., Chapman, S.C., 2016. Velocity of temperature and flowering time in wheat - assisting breeders to keep pace with climate change. Glob. Chang. Biol. https://doi.org/10.1111/gcb.13118

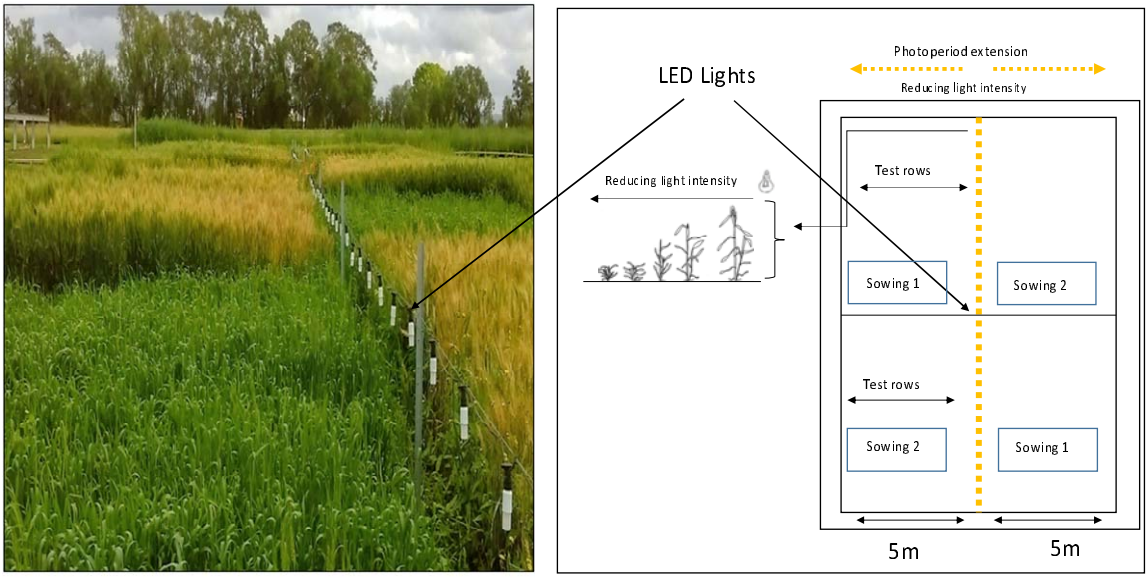

Figure 1: Example layout of the photoperiod extension method (PEM). Wheat genotypes were sown either in a single row (as in this picutre) or in narrow plots. In the centre of the trial at the end of each test row, at the central axis of the experiment, LED lights were setup. These supplemental lights extend the photoperiod to 20 h. The intensity of light diminishes along the row and induces a gradient of flowering times within each test row.

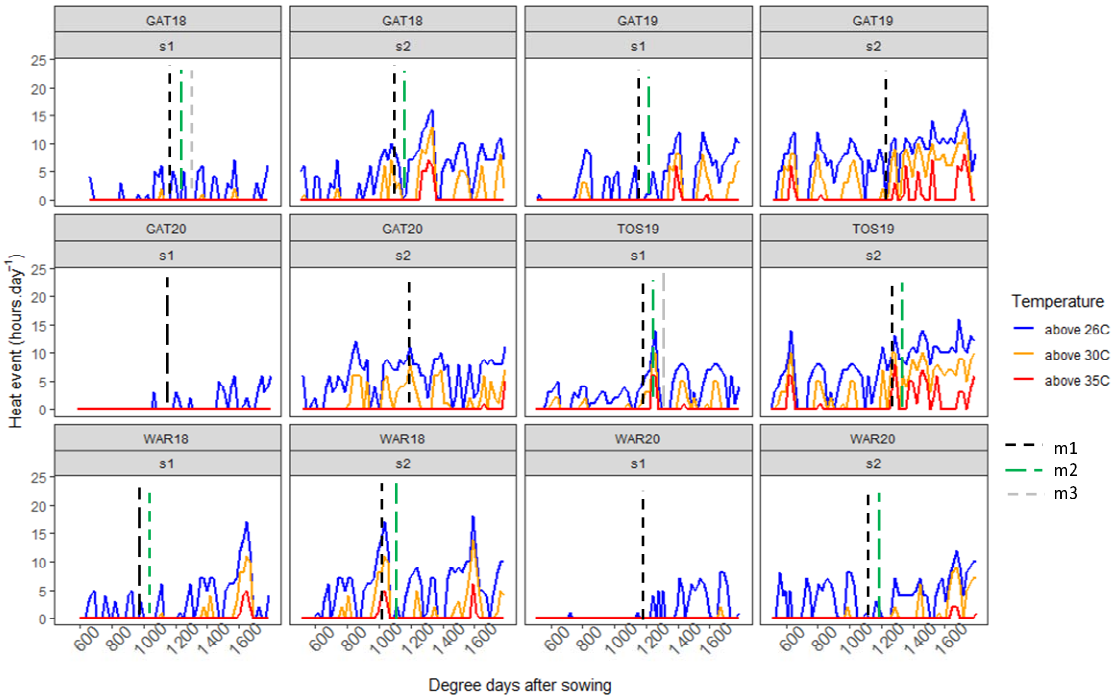

Figure 2: The number of hours each day when air temperatures exceeded 26^{o}C (blue lines), 30^{o}C (orange lines) or 35^{o}C (red lines) is plotted against degree days (^{o}C days) post flowering. These are presented for each location, season and sowing time. The vertical lines represent tagging of wheat genotypes at flowering. m1: 1st coherent of plants tagged at flowering, m2: 2nd coherent of plants tagged at flowering), m3: 3rd coherent of plants tagged at flowering.

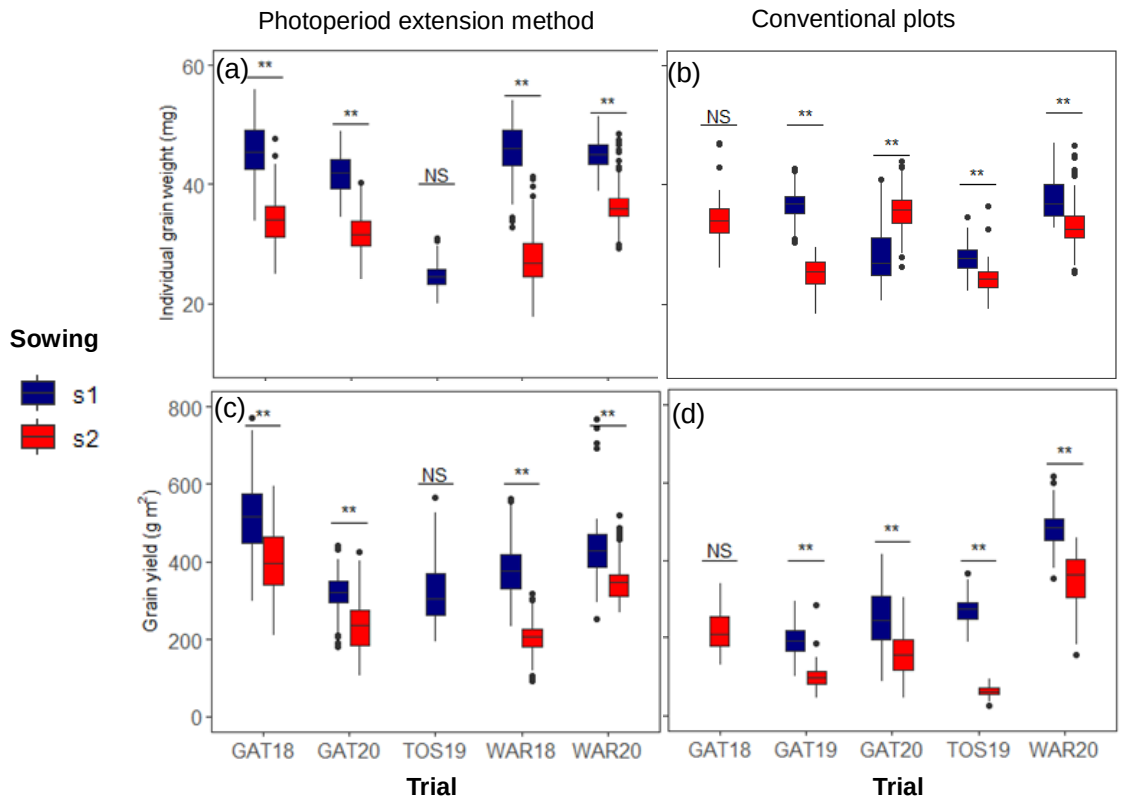

Figure 3: Effect of sowing time on (a & c) individual grain size and (b & d) grain yield of tested wheat genotypes for conventional and photoperiod extension method **(PEM, row-metre harvest)** plots. Each boxplot displays data from 32 genotypes and four independent replicates. TOS19 crops only had supplementary irrigation and experienced a mild post-flowering water stress. Horizontal black lines insides each box denote median values; boxes extend from the 25th to the 75th percentile of each group's distribution of values; vertical extending lines (upper and lower whiskers) indicate variability outside the upper and lower quartiles. Black dots represent outlier values. ** corresponds to significant differences at $P< 0.001$ among the treatments (sowing times) within each trial.

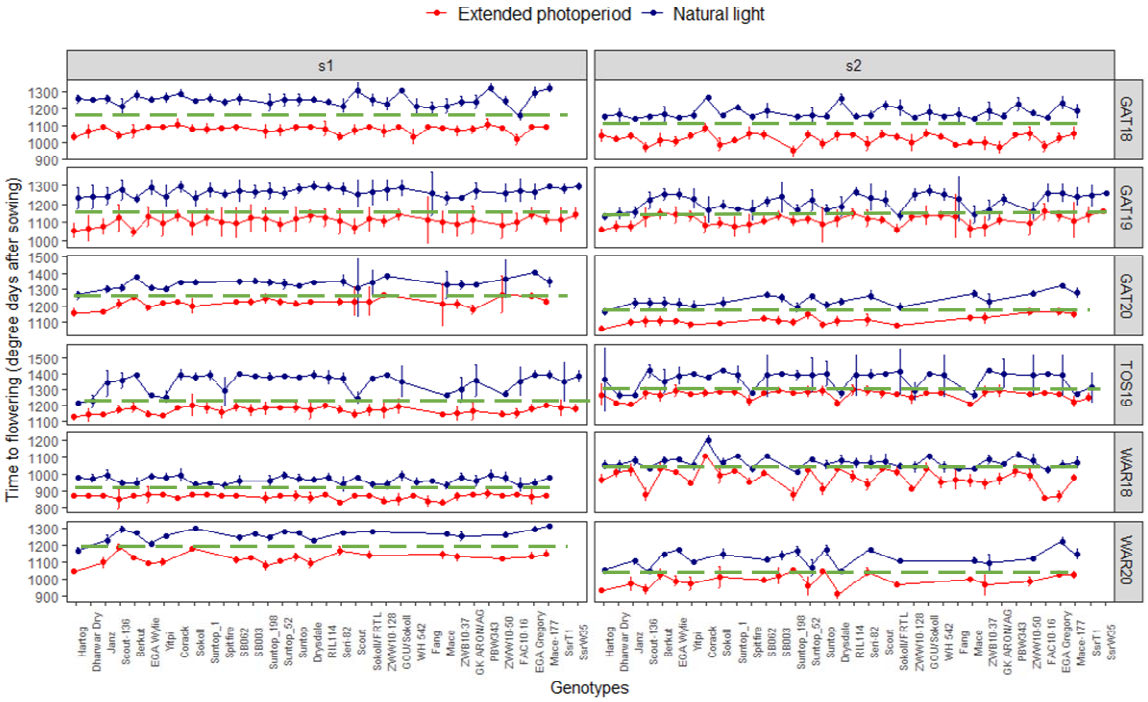

Figure 4: Flowering time of wheat genotypes with and without supplemented light. Horizontal dashed lines correspond to the day of tagging of all wheat genotypes at matched flowering. Data on flowering were collected for plants 0.5 m away from the light source (extended photoperiod) and plants 0.5 m from the end of the row (natural light). Values correspond to the mean of four independent replicates ± confidence interval (95%).

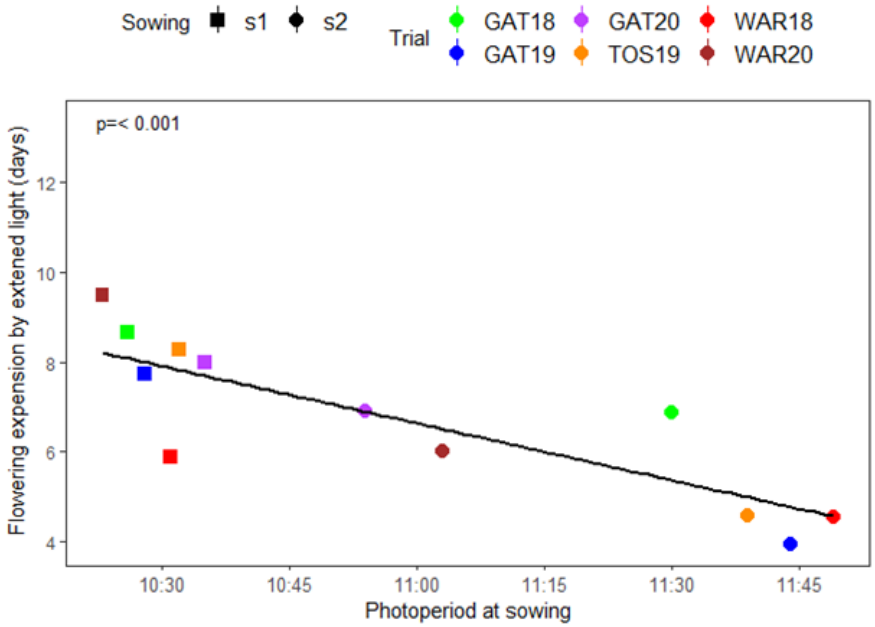

Figure 5: Delay in flowering time due to supplemented light in response to the photoperiod measured at sowing in all trials. The delay in flowering was calculated as the difference in flowering dates for plants located 0.5 m (i.e. extended light, 20 h) and 4.5 m (i.e. natural light) away from the light. Data correspond to the mean of 32 (2018 and 2019) or 20 (2020) genotypes and four independent replicates for all PEM plots. TOS19 crops only had supplementary irrigation and had experienced a mild post-flowering water stress.

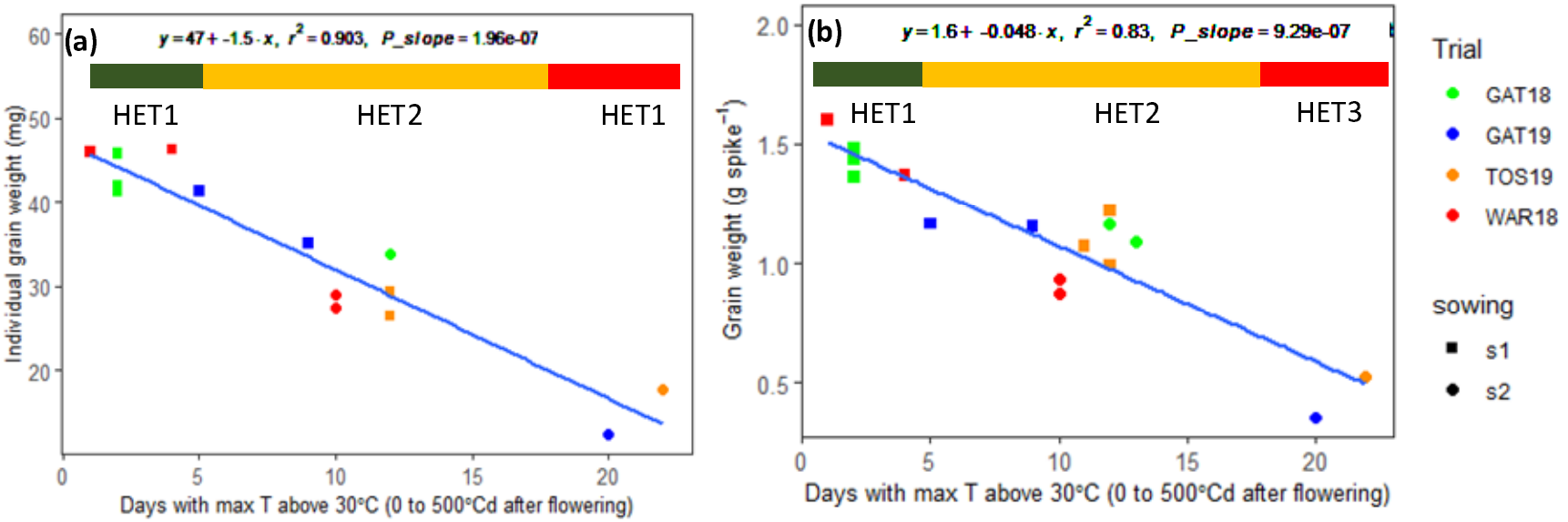

Figure 6: Changes in (a) individual grain weight and (b) spike grain weight, in response to number of post-flowering hot days (0-500^{o}Cd after flowering) across locations and sowing times. Each point represents the mean of all genotypes for individual grain weight of spikes that flowered the same day (four independent replicates of 20 stems each). Environments were classified into heat environment types, HET1, HET2 and HET3, based on the number of post-flowering heat stress days (maximum temperature exceeding 30^{o}C) between 0 and 500^{o}Cd after flowering and indicated by the horizontal bar at the top of each panel. TOS19 crops only had supplementary irrigation and experienced a mild post-flowering water stress.

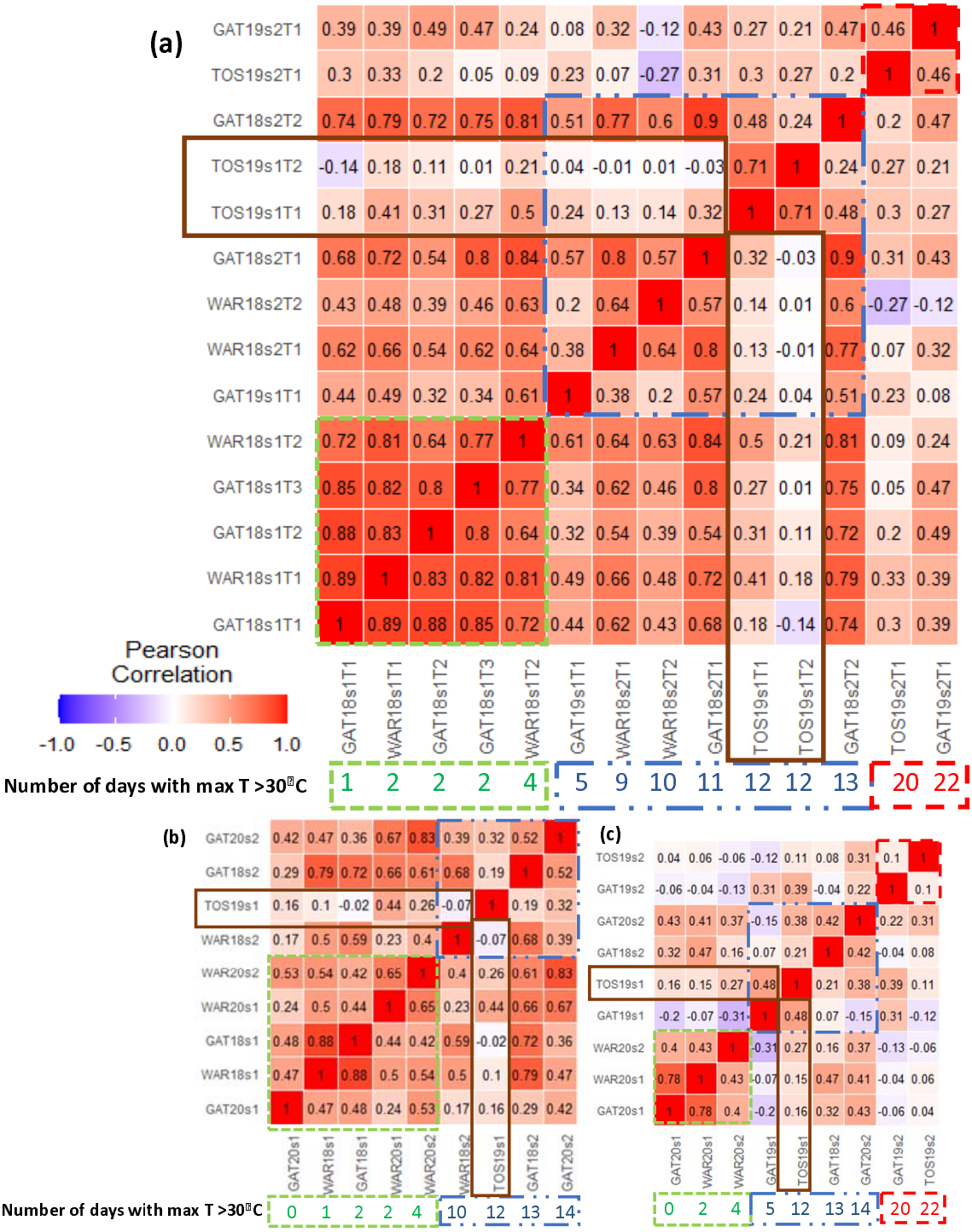

Figure 7: Genetic Pearson's correlation coefficients (r^2) for individual grain weight between environments. Correlations for mean individual grain weight of genotypes between each pair of tested environments. Individual grain weight was estimated from measurements at (a) spike level, and (b) at crop level with row meter harvests in the photoperiod extension method (PEM), as well as at (c) the plot level in the conventional plot trials. Below the heat maps, in blue, are indicated the number post-flowering hot days (days with a maximum temperature above 30°C 0-500°Cd after flowering) for each environment, grouped by heat environment types (HET1, green; HET2, blue; HET3, red, boxes).

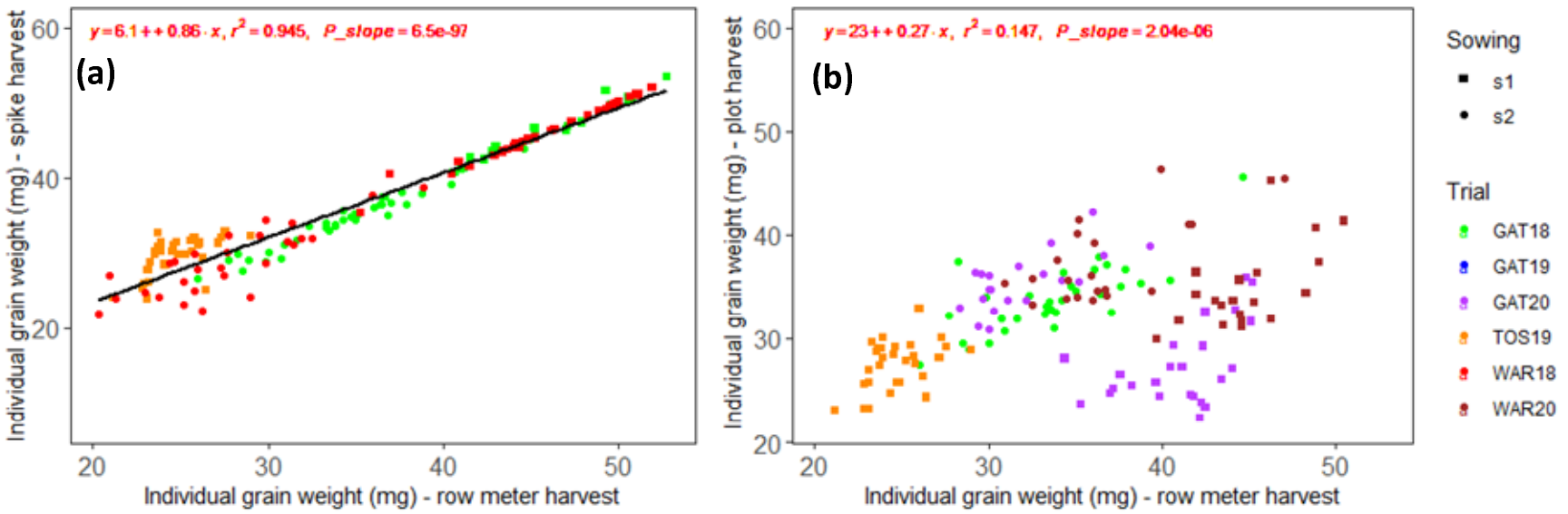

Figure 8: Correlations for individual grain weight of all studied genotypes between (a) data collected from individually tagged spikes and tagged linear row meter at the matched development phase with the photoperiod extension method (PEM), and (b) between conventional yield plots and row meter from PEM. Each data point represents mean value of four independent replicates.

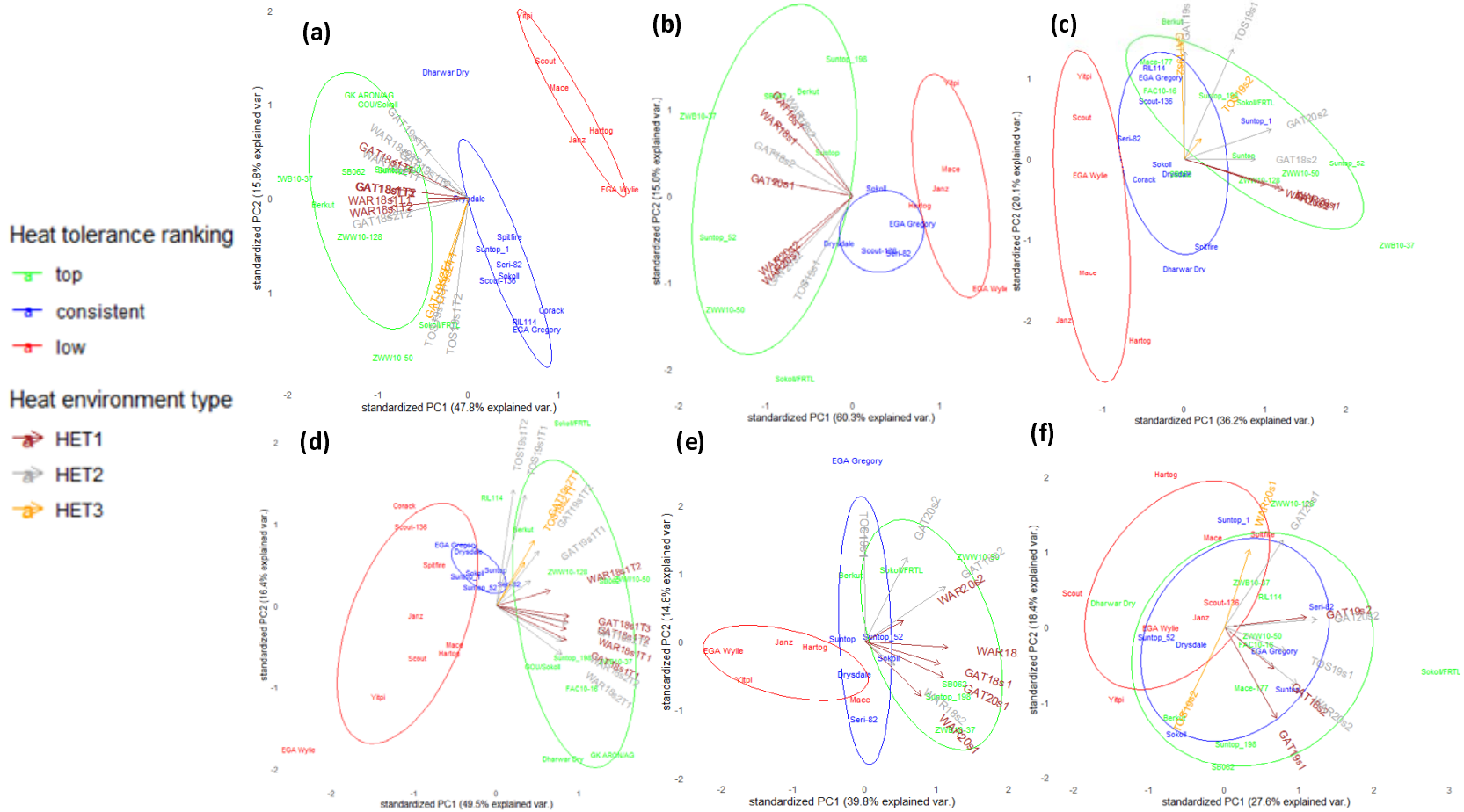

Figure 9**:** Principal component analysis biplot of individual grain weight (a-c) and grain weight per spike (d) or grain yield (e-f) of 32 wheat genotypes for all tested environments. Environments corresponded to combinations of sowing dates and locations (b, c, e, f) together with tagging for single-spike harvests (a, d). Principal component loadings (arrows) were coloured and grouped based on heat environment type i.e. brown: HET1, grey: HET2; orange: HET3. Genotype and eclipse colours correspond to performance of genotypes under different environments i.e. green: top performing genotypes, blue: genotypes with consistent performance across the tested environments; red: genotypes with poor performance across the tested environments.